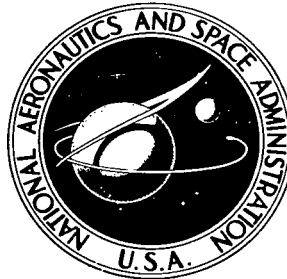


NASA TECHNICAL NOTE



NASA TN D-6009

c. 1

NASA TN D-6009

LOAN COPY: RETU
AFWL (WLOL)
KIRTLAND AFB, TX



TECH LIBRARY KAFB, NM

**MICROASPERITY MODEL FOR
ELASTOHYDRODYNAMIC LUBRICATION
OF A SPINNING BALL ON A FLAT SURFACE**

by Charles W. Allen and Erwin V. Zaretsky

Lewis Research Center

Cleveland, Ohio 44135



0132667

| | | | |
|--|--|--|---------------------------------|
| 1. Report No. NASA TN D-6009 | 2. Government Accession No. | 3. Recipient's Catalog No. | |
| 4. Title and Subtitle MICROASPERITY MODEL FOR ELASTOHYDRODYNAMIC LUBRICATION OF A SPINNING BALL ON A FLAT SURFACE | | 5. Report Date October 1970 | 6. Performing Organization Code |
| | | 8. Performing Organization Report No. E-5758 | 10. Work Unit No. 126-15 |
| 7. Author(s) Charles W. Allen and Erwin V. Zaretsky | | 11. Contract or Grant No. | |
| 9. Performing Organization Name and Address Lewis Research Center National Aeronautics and Space Administration Cleveland, Ohio 44135 | | 13. Type of Report and Period Covered Technical Note | |
| | | 14. Sponsoring Agency Code | |
| 12. Sponsoring Agency Name and Address National Aeronautics and Space Administration Washington, D.C. 20546 | | 15. Supplementary Notes | |
| 16. Abstract A microasperity elasto-hydrodynamic (EHD) model was developed for a ball spinning without rolling on a flat surface. The theory was developed by using a sinusoidal surface model in conjunction with existing dry-contact deformation theory and point-contact elasto-hydrodynamic theory for the microasperities. The computed torques based on this model were compared with experimental torques using the NASA spinning torque apparatus. Fair agreement was obtained between theoretical and experimental results below 300 000 psi maximum Hertz stress. Based on the model presented herein microasperity EHD lubrication does not appear to be a primary force in maintaining separation between the opposing surfaces. | | | |
| 17. Key Words (Suggested by Author(s)) Elastohydrodynamic Microasperity lubrication Rolling-element bearings Lubrication at point contacts Surface roughness | | 18. Distribution Statement Unclassified - unlimited | |
| 19. Security Classif. (of this report) Unclassified | 20. Security Classif. (of this page) Unclassified | 21. No. of Pages 20 | 22. Price* \$3.00 |

MICROASPERITY MODEL FOR ELASTOHYDRODYNAMIC LUBRICATION OF A SPINNING BALL ON A FLAT SURFACE

by Charles W. Allen* and Erwin V. Zaretsky

Lewis Research Center

SUMMARY

A microasperity elastohydrodynamic (EHD) model was developed for a ball spinning without rolling on a flat surface. The theory model was developed by applying to a sinusoidal surface model, existing dry-contact deformation theory and point-contact elastohydrodynamic theory. The computed torques based on this model were compared with experimental torques using the NASA spinning torque apparatus.

There is fair agreement between the theoretical and experimental results below 300 000-psi (207×10^7 -N/m²) maximum Hertz stress although the exponential form of the torque-stress curves differ. Theory would indicate that microasperity EHD lubrication would be most effective where the nominal Hertz stress is low and the sliding velocity is high. Both of these conditions are satisfied at the outer region of the contact circle. This, however, is the region where the first asperity contact does occur if a test is run for long enough duration. Based upon the model presented, microasperity EHD lubrication does not appear to be a primary force in maintaining separation between the opposing surfaces.

INTRODUCTION

There are several factors that can affect ball spinning torque and rolling friction in an angular-contact ball bearing. Some of the parameters which have been reported to affect ball-spinning torque are ball-race conformity, contact stress, and lubricant type (refs. 1 to 5). Other factors that may affect the spinning torque are surface finish, spinning speed, lubricant viscosity, and other lubricant properties.

Much work has been performed to define the lubricant and its behavior in a nonconforming groove where spinning without rolling occurs (refs. 5 and 6). In reference 6

*Associate Professor of Mechanical Engineering, Chico State College, Chico, California.

an elastohydrodynamic (EHD) model was developed. However, it was assumed that some type of lubricant film existed within the center region of contact (fig. 1) within which it was not possible to generate an EHD film. There was good correlation between the analytical and experimental results. However, there were several factors not considered in the analysis which may or may not be of secondary importance. One of these factors is the effect of the surface roughness which may introduce a microasperity lubrication effect. Microasperity lubrication, whether it be hydrodynamic or elastohydrodynamic, in which the deformation and pressure-viscosity effects must be considered, is a phenomenon which, in the general case, must include the shape, size, deformation and distribution of the asperities at the lubricant interface and the interaction between individual asperities. Very little work on the theory of microasperity elastohydrodynamic lubrication has been reported.

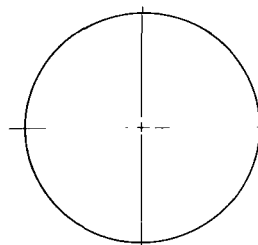
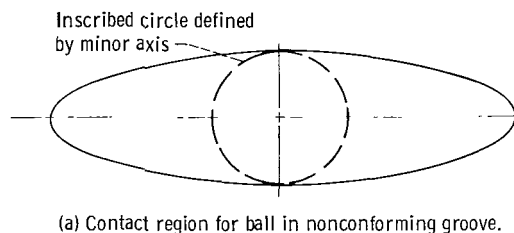


Figure 1. - Contact geometries for ball on nonconforming surface.

Some work has been reported (refs. 7 and 8) in microasperity lubrication in which the viscosity is assumed to be constant and deformation is neglected. Both of the referenced works consider the asperities to be cylinders distributed uniformly on a plane and in nominal contact with another smooth plane. The lubrication of sinusoidal asperities by a viscoelastic fluid was considered in reference 9. Elastohydrodynamic theory has been applied to the collision of two individual asperities (ref. 10). The asperities are

considered to be of parabolic shape and long; therefore, the problem is reduced to a two-dimensional analysis.

The objectives of the work reported herein were (1) to develop a model to describe microasperity elastohydrodynamic lubrication theory for a ball spinning without rolling on a flat surface and (2) to compare the analysis with experimental results. The method of analysis considers first an asperity surface model for dry-contact. Subsequently, an elastohydrodynamic solution is undertaken using point-contact theory for the microasperities. The dry-contact and EHD solutions were then combined into a microasperity elastohydrodynamic theory as suggested in reference 11. The results of this theory were compared to the experimental results reported in reference 2.

SYMBOLS

| | |
|----------------|---|
| A | area, in. ² (m ²) |
| a | radius of contact circle, in. (m) |
| d | distance between two surfaces, in. (m) |
| E | modulus of elasticity, psi (N/m ²) |
| H | Vickers hardness, psi (N/m ²) |
| K | thermal conductivity, Btu/(sec)(ft)(°F); (W/(m)(°C)) |
| l | average distance between asperities, in. (m) |
| M _s | spinning torque, lb-in. (N-m) |
| p | pressure, psi (N/m ²) |
| p ₁ | pressure at which viscosity exponent changes, psi (N/m ²) |
| p _A | average pressure over typical asperity, psi (N/m ²) |
| Q | heat generation, Btu/sec (W) |
| q | heat flux, Btu/(ft ²)(sec) (W/m ²) |
| R | radius of ball, in. (m) |
| r | radius of elemental annulus, in. (m) |
| T | temperature, °F (°C) |
| t | time, sec |
| W | normal load, lb (N) |
| V | entraining velocity (vector sum of surface velocities), in./sec (m/sec) |

| | |
|----------------------|--|
| α, β | pressure-viscosity exponents, psi (N/m^2) |
| κ | diffusivity, in^2/sec (m^2/sec) |
| μ | absolute viscosity, reyns, $\text{lb-sec}/\text{in.}^2$ ($\text{N-sec}/\text{m}^2$) |
| μ_0 | absolute viscosity at entry to contact zone, reyns, $\text{lb-sec}/\text{in.}^2$ ($\text{N-sec}/\text{m}^2$) |
| ρ | radius of curvature, in. (m) |
| σ | composite surface roughness (rms), μ in. (μ cm) |
| σ_1, σ_2 | surface roughness (rms) for surfaces 1 and 2, μ in. (μ cm) |
| σ' | amplitude of sinusoidal surface model, μ in. (μ cm) |
| τ | shear stress, psi (N/m^2) |
| ω | angular velocity, rad/sec |

SURFACE ROUGHNESS

The surface roughness models considered herein were developed for the case of dry-contact and normal approach with no sliding. Sliding under unlubricated conditions would cause shearing and plastic deformation of the asperities. However, if a thin film can be shown to exist between asperities, the shear will take place within this film and the normal approach model would be applicable for a first approximation (ref. 12).

Some of the proposed asperity models are shown in figure 2. The models portrayed may be treated as two-dimensional in which the hemispheres become cylinders, the cones become wedges, etc. They also may be treated three dimensionally.

In reference 13, a sophisticated model is considered. This model consists of hemispherical asperities which have superimposed on them other much smaller hemispherical asperities. The distribution of asperity heights is usually close to Gaussian as reported in reference 14.

Another very important aspect of the contact of rough surfaces is the mode of deformation. Frequently, the deformation is assumed to be elastic or ideal plastic although plastic hardening or elastic-plastic are sometimes considered, as reported in reference 15. It is also shown in reference 15 that, if an exponential distribution is used instead of the more realistic Gaussian distribution, the true area of contact is directly proportional to the load. This is not true for the Gaussian distribution and a particular mode of deformation must be assumed. A true Gaussian distribution requires a finite probability of some plastic and elastic deformation existing together. After repeated contacts have been made, however, the high asperities have all yielded. During subse-

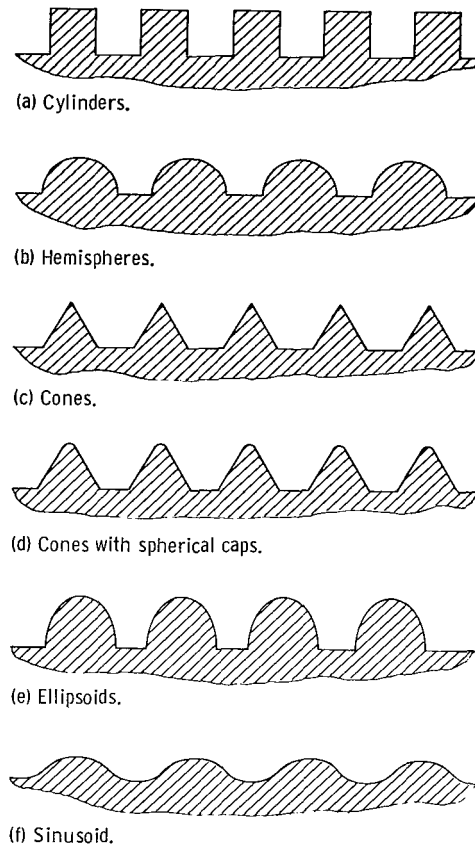


Figure 2. - Surface models.

quent loading, the deformation will be essentially elastic with a load close to that required for plastic deformation.

In all surface contact work it is necessary to distinguish between the nominal and real areas of contact. The following definitions from reference 16 will be used throughout this report:

- (a) Nominal area of contact - the apparent area of overlap of the contacting solids
- (b) Real area of contact - the sum of the separate microscopic areas at which the microasperities are in physical contact

The distribution of load over the nominal contact area will differ from the Hertzian distribution but in reference 17 it is shown that, at high loads, the overall pressure distribution approaches the Hertzian shape.

Much of the previous work on the contact of rough surfaces has considered the contact between a rough surface and a smooth surface. In reference 15 it is shown that, from a statistical viewpoint, the contact of two rough surfaces is the same as that of a rough surface and a smooth surface, provided the roughness on the single rough surface is taken as the composite value given by:

$$\sigma = \sqrt{\sigma_1^2 + \sigma_2^2} \quad (1)$$

where:

- σ composite roughness, (rms)
- σ_1 roughness of surface 1, (rms)
- σ_2 roughness of surface 2, (rms)

For microasperity elastohydrodynamic lubrication, it is the relative distance, d , between the two surfaces which is important (fig. 3). Therefore, the single rough surface with a composite roughness as given above, is deemed to be a sufficiently accurate representation of the real situation.

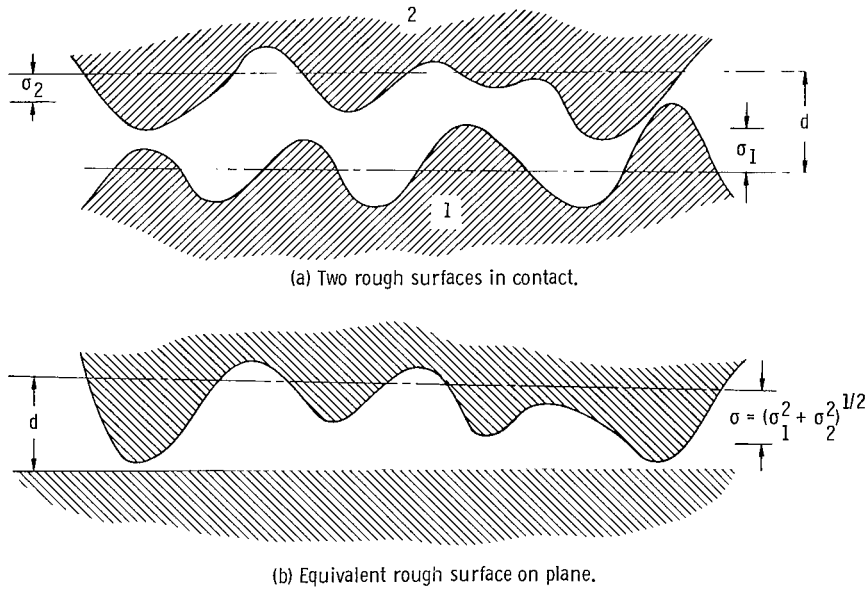


Figure 3. - Surfaces in contact.

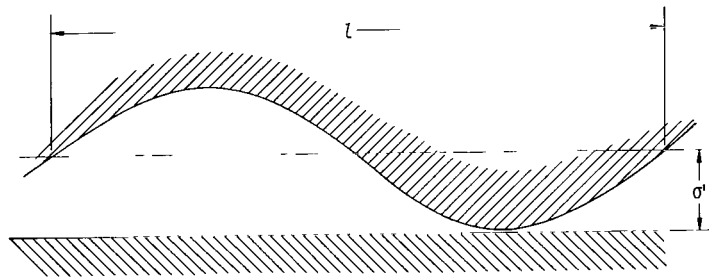


Figure 4. - Sinusoidal surface model.

The surface model which is the most representative of typical bearing surfaces is the sinusoidal model and this will be used in the analysis. A typical sinusoidal asperity sliding against a smooth plane is shown in figure 4. In accordance with the relation between the amplitude and rms values for a sinusoidal waveform, the "amplitude" of this sinusoidal form is taken as $\sqrt{2}\sigma$ and the "wave length" l as the average distance between asperities. The radius of curvature ρ at the peak is then given by

$$\rho = \frac{l^2}{4n^2\sigma'} \quad (2)$$

where

l average distance between asperities

and

$$\sigma' = \sqrt{2}\sigma$$

The load carried by an individual asperity will be computed on the basis that it is close to that at which plastic deformation occurs (ref. 14). In reference 18, curves are given which indicate that for a spherical contact, the onset of plastic flow occurs when the average Hertz pressure reaches about 40 percent of the Vickers Hardness Number. This will be taken as the average Hertz pressure over a typical asperity and is given by:

$$p_A = 0.4 H \quad (3)$$

where

p_H average pressure over typical asperity

H Vickers hardness converted to same units as the average (Hertz) pressure

If the nominal contact between the ball and flat plate is now considered, the true area of contact at a radius r from the center of the nominal circle of contact, radius a , may be determined by considering an elemental annular ring of width dr (fig. 5) and realizing that the nominal force, considering a Hertzian distribution, and the actual force applied through the asperities, are equal.

$$p_A dA = p(2\pi r dr)$$

where

dA elemental area of contact over asperity peaks at radius r , therefore

$$dA = \frac{2\pi r p dr}{p_A}$$

But for a Hertzian contact:

$$p = \frac{1.5 W}{\pi a^2} \sqrt{1 - \left(\frac{r}{a}\right)^2} \quad (4)$$

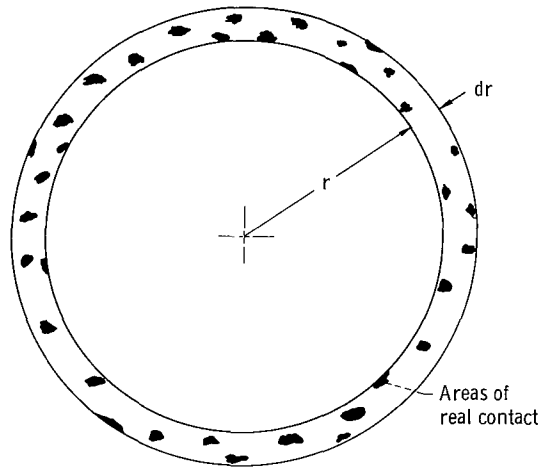


Figure 5. - Elemental annulus showing areas over which force is applied through asperities.

The radius of the nominal contact region a is given in reference 19 as

$$a = 1.109 \sqrt[3]{\frac{WR}{E}} \quad (5)$$

where

W normal load

R ball radius

E modulus of elasticity

a radius of nominal contact region

and

$$dA = \frac{3rW\sqrt{1 - \left(\frac{r}{a}\right)^2} dr}{a^2 p_A} \quad (6)$$

ELASTOHYDRODYNAMIC LUBRICATION AT POINT CONTACTS

Considerable experimental and some analytical work has been performed on point-contact lubrication (refs. 20 to 23). An approximate expression for the film thickness under point-contact conditions is given in reference 21 as

$$h = 0.67(\alpha\mu_0 V)^{2/3} \rho^{1/3} \quad (7)$$

where

- h film thickness
- α pressure-viscosity exponent
- μ_0 viscosity of lubricant at entry to contact zone
- V entraining velocity (vector sum of surface velocities)
- ρ radius of curvature of point contact

While there exists more sophisticated formulas to calculate film thickness, the above simple formula is deemed adequate as a first approximation for a microasperity elastohydrodynamic theory.

SPINNING TORQUE

For an individual asperity as shown in figure 6, the film thickness is given by equation (7). Now, considering all the asperities contained within the annulus of radius r and width dr , the total area of contact is given by equation (6). If the fluid is assumed to behave in a Newtonian manner and the velocity gradient is assumed to be linear, then the shear stress τ in the fluid on the top of the asperities is given by:

$$\tau = \mu \frac{\omega r}{h}$$

where

μ viscosity within lubricating film

ω angular velocity of ball spin about axis perpendicular to contact surface

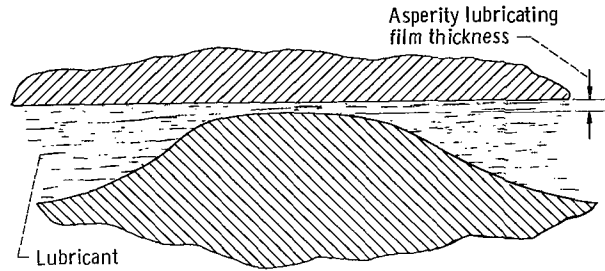


Figure 6. - Mode of asperity lubrication.

The elemental torque imposed by the microasperity film within this annulus is then

$$\begin{aligned} dM_s &= r\tau \, dA \\ &= \frac{\omega\mu r^2}{h} \, dA \end{aligned} \quad (8)$$

where

$$M_s = \text{Torque}$$

In the above equation μ is constant because the pressure over the asperity peaks is assumed constant and, according to the analysis presented in appendix A, isothermal conditions may be assumed to prevail for tests of 15 to 30 seconds duration. For purposes of the model the effect of the fluid lying in the valleys between the asperities is neglected.

The total spinning torque is thus the integral of equation (8) over the whole region of contact.

$$M_s = \omega \int_A \frac{\mu r^2}{h} \, dA$$

Substituting expressions for dA and h from equations (6) and (7), respectively, the spinning moment is obtained as:

$$M_s = \frac{3\omega^{1/3}\mu W}{(\alpha\mu_o)^{2/3}\rho^{1/3}a^2 p_A} \int_0^a \frac{r^3 \sqrt{1 - \left(\frac{r}{a}\right)^2}}{r^{2/3}} dr$$

Integrating this numerically and substituting the value of a from equation (5) the spinning torque is obtained as

$$M_s = \frac{0.89 W^{13/9} R^{4/9} \omega^{1/3} \mu}{E^{4/9} (\alpha\mu_o)^{2/3} \rho^{1/3} p_A} \quad (9)$$

RESULTS AND DISCUSSION

Values of spinning torque were calculated using equation (9) for a ball spinning without rolling on a flat surface using a synthetic paraffinic oil without additives as the lubricant for the following conditions:

| | |
|--|--|
| Speed, rpm (rad/sec) | 1050 (110) |
| Load, lb (N) | 5 to 60 (22 to 267) |
| Maximum Hertz stress, psi (N/m ²) | 160 000 to 370 000 (110×10 ⁷ to 260×10 ⁷) |
| Surface roughness of ball, μ in. (μ cm) rms. | 2 (5.1) |
| Surface roughness of groove, μ in. (μ cm) rms | 3 (7.6) |
| Typical number of asperities per in. (per cm), ref. 16 | 1000 (394) |
| Hardness of ball and flat, Rc | 63 |

Using the above values the composite roughness from equation (1) is found to be approximately 4 microinches (10.2 microcentimeters) rms, and the average asperity tip radius is approximately 0.005-inch (0.012 cm). From equation (3) the average pressure over a typical asperity is 440 000 psi (306×10⁷ N/m²).

The pressure-viscosity relation for a synthetic paraffinic oil (ref. 6) is shown in figure 7 and given as:

$$\mu = \mu_o e^{\alpha p_A} \quad p_A \leq p_1 \quad (10a)$$

$$\mu = \mu_o e^{\left[\alpha p_1 + \beta(p_A - p_1)\right]} \quad p_A > p_1 \quad (10b)$$

where

- α pressure-viscosity coefficient; $9.2 \times 10^{-5} \text{ (psi)}^{-1}$, $(1.33 \times 10^{-8} \text{ (N/m}^2\text{)}^{-1})$
- β pressure-viscosity coefficient; $5 \times 10^{-6} \text{ (psi)}^{-1}$, $(0.72 \times 10^{-9} \text{ (N/m}^2\text{)}^{-1})$
- p_1 critical pressure; 55 000 psi ($37 \times 10^7 \text{ N/m}^2$)
- μ viscosity at entry to asperity contact; 6×10^{-5} reyns (0.4 N-sec/m^2)

Values of torque computed from equation (9) are shown in figure 8 and compared to experimental results from reference 2.

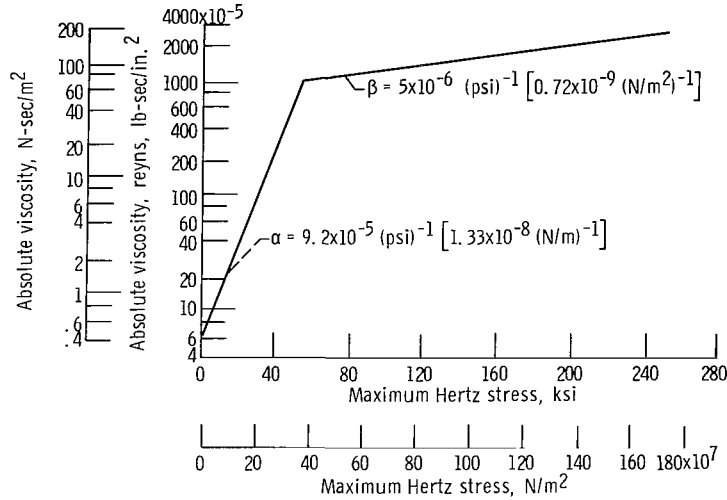


Figure 7. - Theoretical pressure-viscosity relation for synthetic paraffinic oil at 83° F (302 K) (from ref. 6).

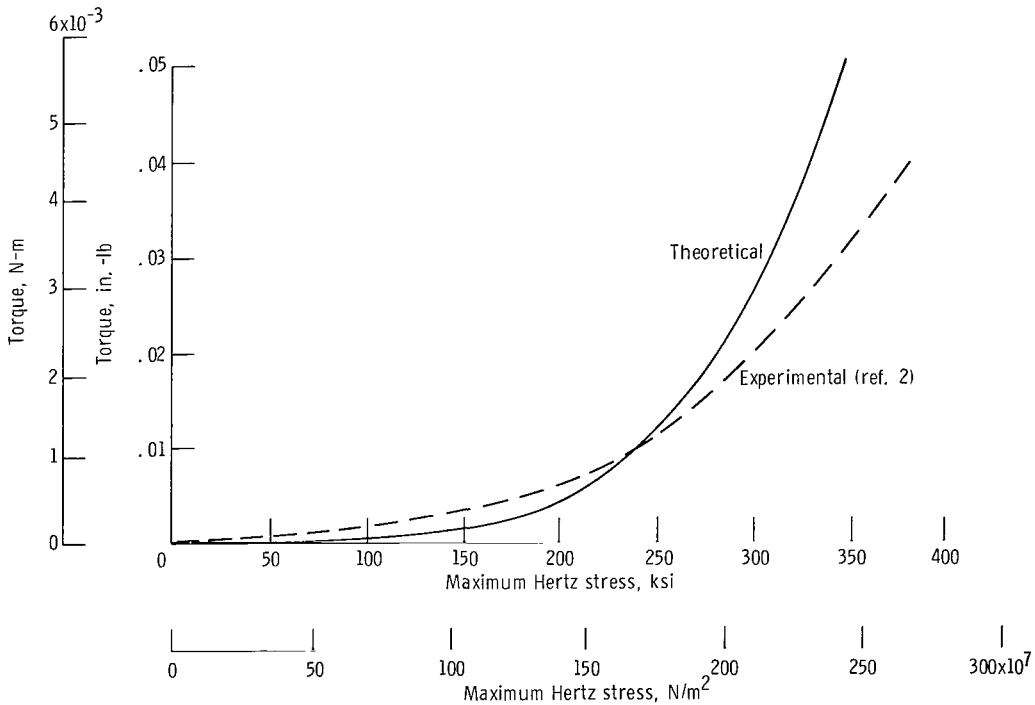


Figure 8. - Torque computed from microasperity EHD analysis compared with that experimentally obtained.

A comparison of the theoretical and experimental results at stress levels below 300 000 psi ($207 \times 10^7 \text{ N/m}^2$) maximum Hertz stress shows them to be in agreement although the exponential forms of the curves differ. The effect of the fluid filling the valleys was ignored in the analysis. However, the torque contribution from this fluid may not be negligible. The exact contribution is dependent upon the viscosity of the fluid within the valleys. This in turn depends upon the pressure, which, for this analysis, was assumed to be atmospheric. The pressure could, however, be much greater. Any increase in the viscosity within the valleys will increase the film thickness over the peaks since the latter is dependent upon the viscosity of the fluid entering the real contact zone. This increased film thickness would reduce the shear stress over the asperities. Thus, the effect of the shear within the valleys may be decreased by the reduced shear force over the tips of the asperities.

The area of real contact over the tips of the microasperities is given as a percentage of the nominal contact area in figure 9. The derivation of this relation is presented in appendix B. From figure 9 it may be seen that at stresses greater than 300 000 psi ($207 \times 10^7 \text{ N/m}^2$) over 65 percent of the nominal contact area is in actual microasperity contact near the center of the nominal contact circle. This traps fluid in "lakes" between the asperities. The resulting squeeze effect would tend to increase the separation of the surfaces. Any increase in film thickness would tend to reduce the torque below the predicted value and this would be more evident at higher loads. Thus, the net effect would be to flatten the torque-stress curve.

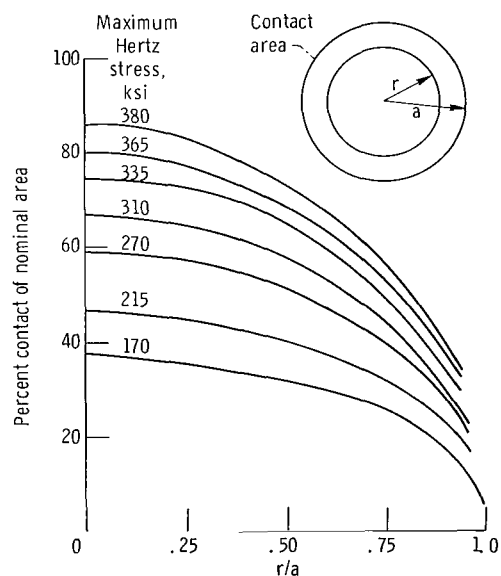


Figure 9. - Asperity contact area as percent of nominal area.

The film thickness between the tips of the asperities and the opposing surface as calculated by equation (7) is about 0.2 microinch ($0.5 \mu\text{cm}$) (50 \AA). This is only a few molecules thick. Therefore, the validity of this analysis depends upon the bulk viscosity of the lubricant remaining unchanged for films a few molecules thick. Direct experimental verification of the viscosity of such thin films appears to be impossible at the present time.

Based upon the assumptions made herein, microasperity EHD lubrication would be most effective where the nominal Hertz stress is low and the sliding velocity is high. Both of these conditions are satisfied at the outer region of the contact circle (fig. 10). This, however, is the region where the first metal to metal contact occurs during test. Therefore, microasperity EHD lubrication does not appear to be a primary force in maintaining separation between the opposing surfaces.

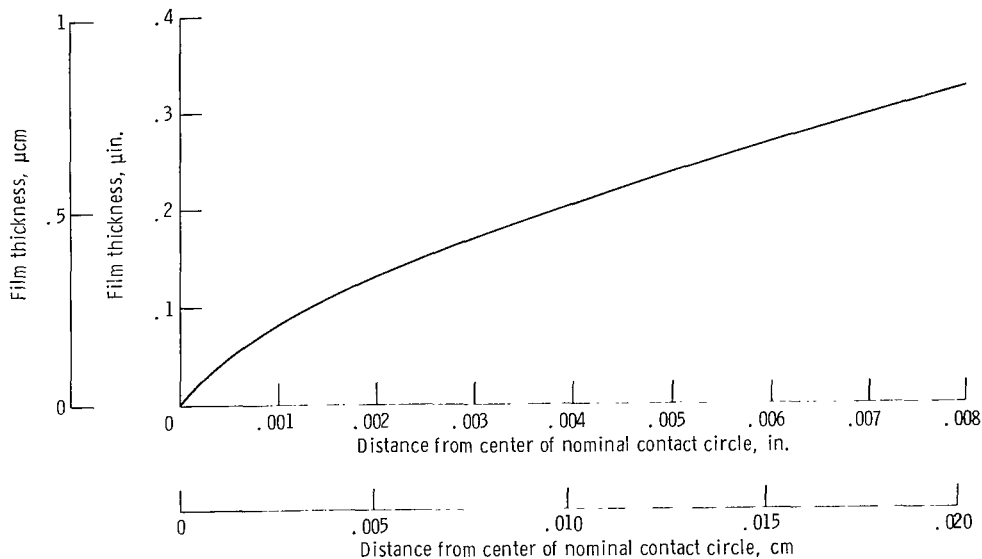


Figure 10. - Theoretical film thickness over microasperities as function of distance from center of nominal contact circle (eq. (7)).

SUMMARY OF RESULTS

A microasperity elastohydrodynamic model was developed for a ball spinning without rolling on a flat surface. The analytical results were compared with experimental results previously obtained. The model assumed sinusoidal asperities model and combined the effects of dry contact deformation, point-contact deformation, and point-contact elastohydrodynamic theory. The following results were obtained:

1. There is agreement between the theoretical and experimental results at stress

levels below 300 000-psi (207×10^7 -N/m²) maximum Hertz although the exponential form of the torque-stress curves differ.

2. Microasperity EHD lubrication would be most effective where the nominal Hertz stress is low and the sliding velocity is high. Both of these conditions are satisfied at the outer region of the contact circle. This, however, is the region where the first asperity contact will occur during test. Based on the model presented herein, microasperity EHD lubrication does not appear to be a primary force in maintaining separation between the opposing surfaces.

Lewis Research Center,
National Aeronautics and Space Administration,
Cleveland, Ohio, June 30, 1970,
126-15.

APPENDIX A

ESTIMATE OF TEMPERATURE RISE AT BALL-PLATE INTERFACE

As an example of the temperature rise at the interface consider the case of a maximum Hertz stress of 300 000 psi ($207 \times 10^7 \text{ N/m}^2$) for which the experimental torque is 0.018 pound-inch (0.00203 N-m).

At a spinning speed of 110 radians per second the heat generated per unit time is

$$Q = \frac{\omega M^2}{9336} = 2.13 \times 10^{-4} \text{ Btu/sec (0.224 W)}$$

The area of the nominal contact circle is

$$A = \pi a^2 = 1.55 \times 10^{-4} \text{ in.}^2 (1.0 \times 10^{-7} \text{ m}^2)$$

If the heat flux is divided equally between ball and plate then the heat flux into either is

$$q = \frac{Q}{A} = 0.69 \text{ Btu/(in.}^2)(\text{sec}) \quad (1.12 \times 10^6 \text{ W/m}^2)$$

From reference 24 the heat flux into a semi-infinite solid over a circle of radius a , with no heat flux across any other boundary yields a maximum surface temperature rise T given by

$$T = \frac{2q \sqrt{\kappa t}}{K} \left[\text{ierfc}(0) - \text{ierfc} \left(\frac{a}{2 \sqrt{\kappa t}} \right) \right]$$

For steel:

$$K = 5.8 \times 10^{-4} \text{ Btu/(sec)(in.)(}^\circ\text{F)} \quad (4.3 \text{ W/(m)(}^\circ\text{C)})$$

$$\kappa = 1.8 \times 10^{-2} \text{ in.}^2/\text{sec} \quad (1.10 \times 10^{-5} \text{ m}^2/\text{sec})$$

Using the foregoing equation and values, after 30 seconds the maximum temperature increase is 10° F (5.6° C). The mean temperature increase would be less than this. Therefore the assumption of isothermal surfaces appears justified.

APPENDIX B

NOMINAL AND REAL AREA OF CONTACT

From equation (6) the elemental area of real contact at radius r is:

$$dA = \frac{3rW\sqrt{1 - \left(\frac{r}{a}\right)^2}}{a^2 p_A} dr$$

The nominal area of contact at this radius is $2\pi r dr$. Therefore:

$$\frac{\text{Real contact}}{\text{Nominal contact}} = \frac{3W\sqrt{1 - \left(\frac{r}{a}\right)^2}}{2\pi a^2 p_A}$$

This ratio expressed as a percentage is plotted in figure 9.

REFERENCES

1. Parker, R. J.; Zaretsky, E. V.; and Anderson, W. J.: Spinning Friction Coefficients with Three Lubricants. *J. Lubr. Tech.*, vol. 90, no. 1, Jan. 1968, pp. 330-332.
2. Dietrich, Marshall W.; Parker, Richard J.; and Zaretsky, Erwin V.: Effect of Ball-Race Conformity on Spinning Friction. NASA TN D-4669, 1968.
3. Dietrich, M. W.; Parker, R. J.; Zaretsky, E. V.; and Anderson, W. J.: Conformity Effects on Spinning Torque and Friction. *J. Lubr. Tech.*, vol. 91, no. 2, Apr. 1969, pp. 308-313.
4. Miller, Steven T.; Parker, Richard J.; and Zaretsky, Erwin V.: Apparatus for Studying Ball Spinning Friction. NASA TN D-2796, 1965.
5. Townsend, Dennis P.; Dietrich, Marshall W.; and Zaretsky, Erwin V.: Speed Effects on Ball Spinning Torque. NASA TN D-5527, 1969.
6. Allen, C. W.; Townsend, D. P.; and Zaretsky, E. V.: Elastohydrodynamic Lubrication of a Spinning Ball in a Nonconforming Groove. *J. Lubr. Tech.*, vol. 92, no. 1, Jan. 1970, pp. 89-96.
7. Hamilton, D. B.; Walowit, J. A.; and Allen, C. M.: A Theory of Lubrication by Microirregularities. *J. Basic Eng.*, vol. 88, no. 1, Mar. 1966, pp. 177-185.
8. Anno, J. N.; Walowit, J. A.; and Allen, C. M.: Microasperity Lubrication. *J. Lubr. Tech.*, vol. 90, no. 2, Apr. 1968, pp. 351-355.
9. Burton, R. A.: Effects of Two-Dimensional, Sinusoidal Roughness on the Load Support Characteristics of a Lubricant Film. *J. Basic Eng.*, vol. 85, no. 2, June 1963, pp. 258-264.
10. Fowles, P. E.: The Application of Elastohydrodynamic Lubrication to Individual Asperity-Asperity Collisions. *J. Lubr. Tech.*, vol. 91, no. 3, 1969, pp. 464-476.
11. Ku, P. M., ed.: Interdisciplinary Approach to Friction and Wear. NASA SP-181, 1968, pp. 358-376.
12. Moore, D. F.: A History of Research on Surface Texture Effects. *Wear*, vol. 13, June 1969, pp. 381-412.
13. Archard, J. F.: Elastic Deformation and the Laws of Friction. *Proc. Roy. Soc. (London)*, Ser. A, vol. 243, no. 1233, Dec. 24, 1957.
14. Greenwood, J. A.; and Williamson, J. B. P.: Contact of Nominally Flat Surfaces. *Proc. Roy. Soc. (London)*, Ser. A, vol. 295, no. 1442, Dec. 6, 1966, pp. 300-319.

15. Greenwood, J. A.: The Area of Contact Between Rough Surfaces and Flats. *J. Lubr. Tech.*, vol. 89, no. 1, Jan. 1967, pp. 81-91.
16. Kragelsky, I. V.; and Demkin, N. B.: Contact Area of Rough Surfaces. *Wear*, Vol. 3, 1969, pp. 170-187.
17. Greenwood, J. A.; and Tripp, J. H.: The Elastic Contact of Rough Spheres. *J. Appl. Mech.*, vol. 89, no. 1, Mar. 1967, pp. 153-159.
18. Tabor, D.: *The Hardness of Metals*. Oxford Univ. Press, 1951, p. 50.
19. Timoshenko, S.; and Goodier, J. N.: *Theory of Elasticity*. Second ed., McGraw-Hill Book Co., Inc., 1951.
20. Archard, J. P.; and Kirk, M. T.: Lubrication at Point Contacts. *Proc. Roy. Soc. (London)*, Ser. A, vol. 261, 1961, pp. 532-550.
21. Archard, J. F.; and Kirk, M. T.: Influence of Elastic Modulus on the Lubrication of Point Contacts. Paper 15 presented at the Inst. Mech. Eng. Lubrication and Wear Group Convention, London, 1963.
22. Archard, J. F.; and Cowking, E. W.: Elastohydrodynamic Lubrication at Point Contacts. *Proc. Inst. Mech. Eng.*, vol. 180, pt. 3B, 1965-66, pp. 47-56.
23. Cameron, A.; and Gohar, R.: Theoretical and Experimental Studies of the Oil Film in Lubricated Point Contact. *Proc. Roy. Soc. (London)*, Ser. A, vol. 291, no. 1427, Apr. 26, 1966, pp. 520-536.
24. Carslaw, H. S.; and Jaeger, J. C.: *Conduction of Heat in Solids*. Second ed., Clarendon Press, Oxford, 1959, p. 264.

NATIONAL AERONAUTICS AND SPACE ADMINISTRATION
WASHINGTON, D. C. 20546
OFFICIAL BUSINESS

FIRST CLASS MAIL



POSTAGE AND FEES PAID
NATIONAL AERONAUTICS AND
SPACE ADMINISTRATION

01U 001 40 51 3DS 70286 00903
AIR FORCE WEAPONS LABORATORY /WLOL/
KIRTLAND AFB, NEW MEXICO 87117

ATT E. LOU BOWMAN, CHIEF, TECH. LIBRARY

POSTMASTER: If Undeliverable (Section 158
Postal Manual) Do Not Return

"The aeronautical and space activities of the United States shall be conducted so as to contribute . . . to the expansion of human knowledge of phenomena in the atmosphere and space. The Administration shall provide for the widest practicable and appropriate dissemination of information concerning its activities and the results thereof."

— NATIONAL AERONAUTICS AND SPACE ACT OF 1958

NASA. SCIENTIFIC AND TECHNICAL PUBLICATIONS

TECHNICAL REPORTS: Scientific and technical information considered important, complete, and a lasting contribution to existing knowledge.

TECHNICAL NOTES: Information less broad in scope but nevertheless of importance as a contribution to existing knowledge.

TECHNICAL MEMORANDUMS: Information receiving limited distribution because of preliminary data, security classification, or other reasons.

CONTRACTOR REPORTS: Scientific and technical information generated under a NASA contract or grant and considered an important contribution to existing knowledge.

TECHNICAL TRANSLATIONS: Information published in a foreign language considered to merit NASA distribution in English.

SPECIAL PUBLICATIONS: Information derived from or of value to NASA activities. Publications include conference proceedings, monographs, data compilations, handbooks, sourcebooks, and special bibliographies.

TECHNOLOGY UTILIZATION PUBLICATIONS: Information on technology used by NASA that may be of particular interest in commercial and other non-aerospace applications. Publications include Tech Briefs, Technology Utilization Reports and Notes, and Technology Surveys.

Details on the availability of these publications may be obtained from:

**SCIENTIFIC AND TECHNICAL INFORMATION DIVISION
NATIONAL AERONAUTICS AND SPACE ADMINISTRATION
Washington, D.C. 20546**